Published in final edited form as:
Biomacromolecules. 2009 July 13; 10(7): 1810–1817. doi:10.1021/bm900240k.

The Effect of Initial Cell Seeding Density on Early Osteogenic Signal Expression of Rat Bone Marrow Stromal Cells Cultured on Crosslinked Poly(propylene fumarate) Disks

Kyobum Kim[1], **David Dean**[2], **Antonios G. Mikos**[3], and **John P. Fisher**[4,*]

[1]Department of Chemical and Biomolecular Engineering, University of Maryland, College Park, MD

[2]Department of Neurological Surgery, Case Western Reserve University, Cleveland, OH

[3]Department of Bioengineering, Rice University, Houston, TX

[4]Fischell Department of Bioengineering, University of Maryland, College Park, MD

Abstract

The intercellular signaling mechanisms among a transplanted cell population are largely determined by the cell population itself as well as the surrounding environment. Changes in cell-to-cell paracrine signaling distance can be obtained by altering cell density, and signal expression of growth factors can be enhanced by auto/paracrine signal transduction. To examine these relationships, we investigated the effect of cell seeding density on viability, proliferation, differentiation, and the endogenous osteogenic signal expression among rat bone marrow stromal cells (BMSCs) cultured on a 2D disk. Rat BMSCs were isolated from rats and then cultured for 8 days on biodegradable poly(propylene fumarate) disks with three different seeding densities (0.06, 0.15, and 0.30 million cells/disk). At day 1, 4, and 8, viability by Live/Dead fluorescent staining, DNA amount, osteogenic differentiation by alkaline phosphatase and osteocalcin mRNA expression, calcium deposition, and osteogenic growth factor mRNA expression were assayed. Osteogenic signal expression was evaluated using quantitative reverse transcriptase-polymerase chain reaction, and signals of interest include bone morphogenetic protein-2, transforming growth factor-β_1, fibroblast growth factor-2, and platelet-derived growth factor-A. The results from this study demonstrate that rat BMSCs were viable over 8 days without being affected by cell density as well as cell proliferation rate and early osteogenic differentiation were stimulated by lower cell seeding density. Most importantly, this study has demonstrated for the first time that the temporal gene expression profiles of endogenous growth factors can be controlled by altering the initial cell seeding density on poly(propylene fumarate) disks. Therefore, our result suggest that changes in the paracrine signal distance by altering cell seeding density may be a useful strategy to optimize the cell-biomaterial construct microenvironments to enhance the osteogenic signal expression.

Keywords

osteogenic signaling; BMP-2; RT-PCR; bone marrow stromal cells; poly(propylene fumarate)

[*]Corresponding Author: John P. Fisher, Ph.D., Fischell Department of Bioengineering, University of Maryland, 3238 Jeong H. Kim Engineering Building, College Park, Maryland 20742, w: 301 405 7475, f: 301 405 0523, jpfisher@umd.edu, web: http://www.terpconnect.umd.edu/~jpfisher.

Introduction

Functional engineering of natural bone tissues involves three fundamental components: (1) parenchymal or progenitor cells which enable lineage-specific differentiation and subsequently express tissue matrix, (2) scaffolds as temporary frameworks to support bone growth, and (3) osteogenic signals such as growth factors to induce bone-forming cell regeneration. The successful conjugation of these principal components is the most critical and challenging problem to develop functional bone replacements.

As a cell source in the tissue engineering field, bone marrow stromal cells (BMSCs) have been extensively investigated since this heterogeneous cell source contains mesenchymal stem cells. These progenitor cells have distinctive characteristics that allow them to be (1) expanded cell numbers by replication *in vitro* and (2) differentiated into a variety of cell types such as osteoblasts, chondrocytes, and adipocytes [1–4]. Since these differentiated cell types can be developed into various tissues and organs, including bone, cartilage, adipose, tendon and ligament, BMSCs are considered as an excellent source for autologous cell therapy and regenerative strategy in tissue engineering research [5–7]. Therefore, BMSC-seeded polymeric scaffolds have been widely utilized to create successful *in vitro* models for bone tissue repair.

As a potential scaffold material, poly(propylene fumarate) (PPF) is known to be injectable, *in situ* polymerizable, and a biocompatible linear polyester [8]. This polymer contains carbon-carbon double bonds that allow constructs of cross-linked networks, and ester linkages that allow for hydrolytic degradation [9]. PPF degradation products, including propylene glycol, poly(acrylic acid-co-fumaric acid), and fumaric acid, do not shift pH to a level that is hazardous to natural tissues, and can be metabolized as a constituent of the Krebs cycle [9]. PPF can be crosslinked by ultraviolet (UV) radiation with the aid of a photoinitiator such as bis(2,4,6-trimethylbenzoyl) phenylphosphine oxide [10]. PPF also possesses sufficient mechanical strength for use as a bone substitute at load bearing sites [11]. A series of studies have revealed that PPF is a promising biomaterial for bone tissue engineering. It has been used for fabrication of composite materials [12–16], rapid prototyping using laser-stereolithography to create controllable microarchitecture for patient-specific bone implants [17–19], and growth factor delivery vehicles [20, 21].

Lineage-specific differentiation of BMSCs on polymeric scaffolds is correlated with the activation of inductive signaling molecules such as various cytokines, hormones, and growth factors. In order to establish the optimal fabrication parameters necessary for successful bone tissue engineering scaffolds, we propose that it is critical to understand the intercellular signaling mechanisms among the transplanted cell population. Our overall hypothesis is that the proper microenvironment could facilitate osteogenic signals among a transplanted cell population, and paracrine cell-to-cell distance is one of the critical parameter which is determined by initial cell seeding density.

The artificial microenvironment of a cell population seeded on a synthesized polymeric material may facilitate osteogenic signals. A strong understanding of these signaling profiles may be critical to the successful development of a functional cell/scaffold construct. There have been several recent studies to investigate the effect of cell seeding density on cellular activities. Rat bone marrow stromal cells (BMSCs) on three dimensional (3D) poly(DL-lactic-co-glycolic acid) scaffolds showed rapid proliferation at a lower seeding density over the first 7 days, but no changes in osteoblastic functions such as alkaline phosphatase (ALP) activity and mineralization after 56 days in culture [22]. However, increasing the seeding density of rat BMSCs in titanium fiber mesh had a positive effect on osteogenic expression [23] and a higher seeding density on polystyrene well plate led to higher ALP

activity and more mineralization [24]. In addition, an optimal seeding density was determined to best promote intracellular signals, such as Runx2, in MG-63 cells cultured within dense 3D collagen gels [25]. Similarly, a recent study also demonstrated the existence of the minimum and optimum cell seeding density in 3D hydroxyapatite/tricalcium phosphate (TCP) scaffolds for bone yield (i.e., bone contact and bone area) in a goat *in vivo* model [26]. However, another study reporting a contrary result, found that a lower seeding density of human alveolar osteoblasts on 3D polycaprolactone/TCP was associated with higher ALP activity and osteocalcin (OC) secretion [27]. Despite of the fact that there have been many studies about the effect of adding growth factors (i.e., exogenous signals) on the osteogenic differentiation of BMSCs [28–31], changes in endogenous gene expression of signaling growth factors caused by altering the intercellular paracrine communication distance have not been extensively studied. Therefore, the objectives of the present study were to determine the effect of initial seeding density of rat BMSCs onto two dimensional (2D) PPF disks on cell viability, proliferation, and differentiation, as well as to describe the effect of cell seeding density on osteogenic signal expression profiles. Most critically, this study demonstrates for the first time that the expression profiles of endogenous osteogenic growth factors can be controlled by the initial cell seeding density on PPF disks.

Experimental Section

Materials

Diethyl fumarate, propylene glycol, zinc chloride, hydroquinone, ascorbic acid, β-mercaptoethanol, and Alizarin Red S were obtained from Sigma-Aldrich (St. Louis, MO). Analytical reagent grade methylene chloride was purchased from Fisher Scientific (Pittsburgh, PA). Polystyrene standards were received from Polymer Laboratories (Amherst, MA). Bis(2,4,6-trimethylbenzoyl) phenylphosphine oxide (BAPO) was obtained from Ciba Specialty Chemicals (Tarrytown, NY). Alpha-minimum essential medium (α-MEM), penicillin/streptomycin antibiotics, fetal bovine serum (FBS), and trypsin/EDTA were purchased from Invitrogen (Carlsbad, CA). PicoGreen assay kit was obtained from Molecular Probes. Collagenase-P was purchased from Roche (Indianapolis, IN). RNeasy Mini plus kit was received from Qiagen (Valencia, CA). High Capacity cDNA Archive kit, Universal PCR Master mix (2x), and Taqman® Gene Expression Assay for growth factors and osteogenic differentiation marker were purchased from Applied Biosystems (Foster City, CA).

PPF Synthesis and PPF Disk Fabrication

PPF was synthesized with diethyl fumarate and propylene glycol following a two step procedure [8, 10]. Briefly, 1 mol of diethyl fumarate and 3 mol of propylene glycol were reacted with 0.01 mol of zinc chloride as a catalyst and 0.002 mol of hydroquinone as a crosslinking inhibitor with nitrogen gas purge, heat supply, and mechanical stirring. The resulting diester intermediate, bis(2–hydroxypropyl) fumarate, underwent transesterification with vacuum, heat supply, and mechanical stirring until the desired molecular weight was obtained. The final PPF polymer was dissolved in methylene chloride for further purification. The PPF/solvent mixture was purified during serial washing steps with 5 v/v% HCl solution, water, and brine. Residual methylene chloride was evaporated using a rotor-evaporator and vacuum pump. Then, hydroquinone was removed by ethyl-ether precipitation on ice, and excess ethyl ether was completely evaporated again using a rotor-evaporator and vacuum pump. Gel permeation chromatography (GPC) was used to measure the molecular weight and polydispersity index (PDI) of purified PPF. Polystyrene standards with a peak molecular weight of 580, 1180, 2360, and 4490 g mol^{-1} were used to create a calibration curve. The resulting number average molecular weight (Mn) was 2100 g mol^{-1} and PDI was 2.4. For the photocrosslinked disk fabrication, the photoinitiator BAPO was

employed (0.5 g BAPO/g PPF) for photocrosslinked disk fabrication. A homogeneous 1.5 mm thick PPF/BAPO mixture was placed between the glass plates. After 2 hr of ultraviolet (UV) radiation exposure (intensity of 2.68 mW/cm^2), a crosslinked sheet of PPF was retrieved and cut into disks that were 18 mm in diameter and 1.5 mm thick.

Rat Bone Marrow Stromal Cell Isolation and Culture

Rat BMSCs were isolated from femora and tibiae of young male Wistar Hanover rats (101–125g, Taconic, Hudson, NY) following a University of Maryland approved IACUC animal protocol (R-07-94). Following euthanasia by carbon dioxide gas, the femora and tibiae were excised and all soft tissues were removed. The explanted bones were incubated in 10 ml of cell culture medium for 10 min three times. The culture medium contained α-MEM supplemented with 10 % (v/v) penicillin/streptomycin antibiotics, 10 % (v/v) FBS, 0.2 mM of ascorbic acid. Both ends of each bone were clipped off and bone marrow was flushed out with 10 ml of culture media using a syringe and 18-gauge needle under sterile conditions. The collected marrow was homogenized by mixing with a syringe, passed through a 70 μm cell strainer, and centrifuged at 500 g for 5 min. The resulting cell pellets were resuspended with 5 ml of culture media and plated in T-25 cell culture flasks. The media was first changed to remove non-adherent cells after 48 hrs, and changed every 2–3 days over the course of each subculture periods. When 80 % confluency of the cells was reached, cells were enzymatically lifted using trypsin/EDTA. The cells were passaged every 5–7 days until the proper cell number was obtained for further cell seeding. All flasks were incubated under standard cell culture conditions (37°C and 5% CO_2 gas).

Cell Seeding

The PPF disks were prewashed before cell seeding in the following manner: All disks were soaked first in phosphate buffered saline (PBS) for 15 min to eliminate surface debris, second in acetone for 3 min to remove any unreacted monomers, and, third in PBS again for 30 min. After these washing steps, the samples were sterilized with UV radiation in a biosafety laminar flow hood overnight. Each disk was placed in a 12 well tissue culture polystyrene (TCPS) plate. Next, autoclaved stainless steel rings (outer diameter: 19 mm, inner diameter: 16 mm, height: 15mm) were placed onto each disk to confine the cell seeding area, to prevent the disk from floating, and to inhibit the loss of cells at the periphery between the disk and the well. Second passage rat BMSCs were trypsinized from culture flasks and the total cell number was counted using a hemacytometer to calculate the required volume of media for resuspension. After centrifugation, the cell pellet was resuspended with osteogenic media (control media supplemented with 10 mM Na-β-glycerophosphate and 10^{-8} M dexamethasone) to create a series of cell density (0.06, 0.15, 0.30 million cells/200 μl suspension). All of the experimental groups are listed in Table 1. Next, 200 μl of suspension was dropped onto the center of the PPF disks in the stainless steel ring, and 1800 μl of osteogenic media was added to the outer region between the ring and the well (Day 0). The same volume of cell suspension with 0.06 and 0.30 million cells was dropped into a TCPS well plate without a PPF disk as a positive control sample. The cell/disk constructs were incubated for 24 hrs to allow complete cellattachment. The steel rings were removed and the osteogenic media was changed every 2–3 days during the experimental time periods. All the assays except the cell viability test were performed at day 1, 4, and 8.

Cell Viability

Cell viability was examined using a Live/Dead viability/cytotoxicity assay kit to evaluate the initial cell attachment to PPF disks and the viability at day 1 and 8. Osteogenic media was removed from the well and the cell/disk constructs were rinsed with PBS two times to remove unattached cells. Each construct was labeled with 700 μl of calcein AM (2 μM) and

ethidium homodimer-1 (4 μM) fluorescent dye/PBS solution per well. After 30 min incubation at room temperature, images were taken to observe the cell attachment, localization, and viability over the culture periods under a fluorescence microscope (Axiovert 40 CFL with filter set 23, Zeiss, Göttingen, Germany) equipped with a digital camera (Diagnostic instruments 11.2 Color Mosaic, Sterling Heights, MI).

DNA Quantification

To assess cellular proliferation, DNA was isolated and the double-strand DNA amount was quantified using a PicoGreen assay kit. After removing the culture media from the well, the cell/disk constructs were washed with PBS two times. Cell layers on the disks were lifted with 600 μl of trypsin/EDTA, and 600 μl of collagenase-P was added to disrupt the extracellular collagen matrix. After transferring 1200 μl of cell suspension to a new sterile tube, each disk was rinsed with 600 μl of culture media and then transferred to the same tube. Calcein AM staining, and specifically the lack of any stain, was utilized to confirm that all cells had been removed from the disk. A 1,800 μl suspension was centrifuged down (1,000 g, 5 min) to form a cell pellet. After aspirating the supernatant, 1 ml of autoclaved distilled water was placed in each tube and the pellet was homogeneously resuspended. DNA was extracted from the suspension by 3 cycles of freeze (30 min at −80°C), thaw (30 min at 37°C), and sonication in a bath sonicator (30min). After cell-lysis, the cell debris was pelleted by centrifugation at 12,000 g for 10 min and 900 μl of supernatant was transferred to a new sterile tube. Next, 100 μl of supernatant containing DNA was mixed with 100 μl of diluted PicoGreen fluorescent dye in a 96 well plate. The samples in the well plate were incubated for 10 min at room temperature. Fluorescent intensity was recorded at 490 nm of excitation and 520 nm of emission using a M5 SpectraMax microplate reader (Molecular Devices, Sunnyvale, CA). The final double strand DNA amount was calculated based on an λ-DNA standard curve with known DNA concentrations.

RNA Extraction

Total RNA was isolated from each cell/disk construct with a RNeasy Mini plus kit following the protocol provided by the manufacturer. First, cells were lifted and collected in the same manner described above. Once the cell pellet was obtained, 350 μl of RLT lysis buffer with 3.5 μl of β-mercaptoethanol was added. Cells were homogenized by mixing within a 1 ml syringe using a 22 gauge needle. Genomic DNA was removed by passing the lysate through a genomic DNA elimination membrane column. After several washings in a spin column, total RNA was captured by a RNeasy mini-column membrane and eluted with 33 μl of Rnase-free water. RNA concentration and purity were assessed using Nanodrop UV/Vis spectrophotometry (Nanodrop Technologies, Wilmington, DE) with absorbance at 260 and 280 nm.

Quantitative Reverse Transcription Polymerase Chain Reaction (qRT-PCR

Isolated total RNA was reverse transcribed to complementary DNA (cDNA) using the High Capacity cDNA Archive kit. The cDNA sample was subsequently mixed with Universal PCR Master mix (2x) and Taqman® Gene Expression Assays. Four target growth factor genes including bone morphogenic protein-2 (BMP-2, Taqman Assay ID: Rn00567818_m1), transforming growth factor-β1 (TGF-β1, Rn00572010_m1), platelet-derived growth factor-A (PDGF-A, Rn00709363_m1), and fibroblast growth factor-1 (FGF-1, Rn00563362_m1), as well as two osteogenic differentiation marker genes, including ALP (Rn00564931_m1) and osteocalcin (OC), were assessed for relative gene expression level profiles. Pre-developed 18s ribosomal RNA was used as an endogenous control gene. The oligonucleotide primer and Taqman probe sequences for OC were 5’ GGCTTCCAGGACGCCTACA 3’ (forward primer), 5’ GGGCAACACATGCCCTAAAC 3’ (reverse primer), and 5’ CGCATCTATGGCACCAC 3’ (probe). Real time quantitative

polymerase chain reaction (qRT-PCR) was performed on an ABI Prism 7000 sequence detector (Applied Biosystems). The thermal conditions for the PCR were 2 min at 50°C, 10 min at 95°C, and 50 cycles of 15 s at 95°C and 1 min at 60°C. The relative gene expression level of genes of interest (fold change) was first normalized to the mean of 18s control gene data in each group. The TCPS Min group was chosen as a calibrator and fold change was calculated by ΔΔCt method using the mean of the calibrator data. Mean of fold changes compared to the calibrator group (The TCPS Min group) and standard deviations are reported (n=3).

Mineralization Assay

Calcium mineralization was first qualitatively measured by Alizarin Red S staining and light microscopic images. Generally, Alizarin Red S stains calcium deposition orange-red and indicates mineralization of tissues or cells. At day 8, the cell layer on the PPF disk was washed with PBS two times and fixed with 4% paraformaldehyde for 10 min at 4 °C. The fixed cells were stained with 700 μl of 0.5 % Alizarin Red S/PBS solution (pH 4.2) for 10 min at room temperature, washed with PBS 5 times, and observed under an inverted light microscope to verify the presence of a red-colored calcium deposit. Images with x100 magnification were taken from three different spots on each construct (i.e., one in the center and two at the corners, which were 5.66 mm away from the center along a diagonal axis) to quantitatively assess the images. A total of 9 images were obtained from each PPF group (six from the TCPS group). Each image (1.5×1.1 mm^2 dimension at a resolution of 1600 ×1200 pixels) was exported to the ImageJ program. After the subtraction of the background image, all images were converted to black and white binary images. The total black area was automatically calculated. The result was normalized with the DNA amount and presented as total mineralized area per DNA amount.

Statistical Analysis

In order to demonstrate the reproducibility of the data, all experimental groups were analyzed with biological triplicates, and all control groups were analyzed with biological duplicates. In addition, all measurements were collected in triplicate (technical triplicates). The data from all experiments were analyzed by one-way analysis of variance (ANOVA) and Tukey's multiple-comparison test was performed to verify the statistical difference between the experimental groups with 95% confidence ($p < 0.05$). The means and the standard deviations are reported in each figure.

Results

Attachment, Viability, and Differentiation of rat BMSCs

The initial cell attachment, cell distribution, and viability of the rat BMSCs over 8 days were demonstrated by Live/Dead fluorescent staining (Figure 1). Compared to the TCPS positive control, rat BMSCs showed the same initial attachment pattern and distribution throughout the seeding area (Figure 1A). Cells were spread and exhibited cuboidal morphological changes (Figure 1B); few non-viable cells were found in any of the experimental groups at any time points. It was qualitatively demonstrated that as the culture period (i.e., 8 days) progressed, the cells proliferated to cover more surface area of the PPF disks, eventually initiating direct contact between adjacent cells. In addition, rat BMSCs were viable for 8 days in all density groups, implying that the PPF biomaterial provided a suitable 2D substrate.

As measured by DNA content, rat BMSCs proliferated on the surface of PPF disks over the 8 day period in all cell density groups (Figure 2). Except for the PPF Max group, all groups on days 4 and 8 contained a significantly higher DNA amount than at previous time points.

The rate of proliferation in the PPF Min group was highest among the three different density groups, and this observation was in agreement with the qualitative fluorescent images in Figure 1. On the other hand, the PPF Max group displayed minimal proliferation during the first 4 days of culture. These results demonstrated that the lower cell seeding density stimulated more rapid proliferation and that PPF disks can support the rat BMSCs proliferation as a 2D monolayer substrate.

ALP mRNA expression (Figure 3) in the PPF groups showed no significant differences on either day 1 or day 4. ALP expression in the TCPS groups peaked on day 4 and was downregulated on day 8. The lower cell seeding density group (TCPS Min) exhibited higher ALP expression than the higher cell seeding density group (TCPS Max) on day 4. On day 8, the PPF Med group showed statistically higher ALP expression than the Min or Max PPF groups ($p=1.75 \times 10^{-10}$). This ALP mRNA expression pattern at the last time point of day 8 was recorded in all four growth factors. PPF Min and PPF Med groups showed an increase from the initial level of expression by day 4 and this level remained constant until day 8, while ALP expression of PPF Max peaked on day 4 and was more than one-fourth down-regulated on day 8.

In Figure 4, all three PPF density groups had similarly low levels of OC expression on day 1. By day 4, the PPF Max group exhibited a higher expression level than all of the other groups. On day 8, there was no significant difference in OC expression between different cell densities on PPF, while TCPS Max showed higher OC expression than TCPS Min and all three PPF groups. All three PPF groups showed an initially constant level of OC expression level that increased when next observed on day 8 (i.e., approximately a two-fold increase compared with day 1). This trend was also observed for the two TCPS groups, where the OC expression level in the TCPS Max group on day 8 was more than nine times that of day 1.

Calcium deposition was assessed by (1) qualitative microscopic images of Alizarin Red S stained specimens, and (2) subsequent quantitative image analysis (Figure 5). The images of stained calcium deposition indicate that all density groups cultured in osteogenic-supplemented media for 8 days demonstrated mineralization, with higher cell density groups of both the PPF and TCPS substrates showing more extensive mineralization (Figure 5A). Data in Figure 5B confirmed the qualitative assessment of the images shown in Figure 5A by showing that the PPF Med and Max groups had significantly larger mineralized areas than were seen in the PPF Min group specimens. Similarly, TCPS Max was found to have a significantly larger area of calcium deposition than was seen in the TCPS Min group.

Osteogenic Signal Expression

The BMP-2 expression of the PPF Min and Med groups were statistically higher than both the PPF Max and TCPS groups on day 1 ($p = 1.60 \times 10^{-7}$) . The PPF Min and Med groups showed a 4-fold downregulation in BMP-2 expression from day 1 to day 4 (Figure 6A). On day 8, the BMP-2 results demonstrated that both the PPF Min and Med groups exhibited significantly higher BMP-2 expression than did the PPF Max samples ($p = 1.60 \times 10^{-5}$), a result that was similar to what was seen on day 1. BMP-2 expression by rat BMSCs on PPF disks was seen to decrease between days 1 and 4 and then, except for PPF Max, to increase by day 8. Consistent BMP-2 expression over 8 days was observed in All TCPS groups.

Figure 6B represents rat BMSC expression of FGF-2. The PPF Max group exhibited a statistically higher level of FGF-2 expression on day 4 versus the PPF Min and Med groups ($p = 3.46 \times 10^{-4}$). The TCPS Min group showed a higher level of FGF-2 expression than all of the other groups at the day 1 and 4 time points. On day 8, all three PPF groups exhibited higher FGF-2 levels of expression than both TCPS groups. The levels of FGF-2 expression

in the PPF Med group were higher than that seen in all of other experimental groups ($p = 3.35 \times 10^{-8}$).

TGF-β_1 expression exhibited a similar pattern to PDGF-A (Figures 6C and 6D). The expression of both TGF-β_1 and PDGF-A in both TCPS groups peaked on day 4, followed by a more than one-fifth fold decrease between day 4 and day 8. The PPF Med and PPF Max groups showed higher TGF-β_1 expression on day 1 than the PPF Min group, while the PPF Max group showed higher TGF-β_1 expression than the other two PPF groups on day 4. The PPF Med group had significantly higher TGF-β_1 expression than all other groups on day 8 ($p= 3.85 \times 10^{-9}$). Overall, rat BMSCs on PPF disks showed decreasing TGF-β_1 expression over 8 days, with a lower expression level than the TCPS groups by day 4. The data in Figure 6D indicates that the PDGF-A levels presented an expression profile similar to the TGF-β_1 expression profile. While the TCPS Min group exhibited a higher PDGF-A expression level than the TCPS Max group at all time points, both the PPF Min and PPF Med groups showed significantly higher levels of expression than the PPF Max group on day 1 only ($p=1.03 \times 10^{-3}$). By day 4, there was no significant difference in PDGF-A expression between all three PPF groups, but the PPF Med group showed a higher level of PDGF-A expression on day 8 than the other two PPF groups ($p=3.99 \times 10^{-6}$). Sustained expression levels were observed in all three PPF groups over the 8 days; however PDGF-A expression levels of rat BMSCs on the TCPS substrate peaked on day 4 and then decreased on day 8.

Discussion

Intercellular signaling via endogenous signal molecules among a transplanted cell population may be determined as much by the cell population itself as by the surrounding environment. To mimic a natural bone healing environment, and to optimize the components for an engineered bone substitute, it is of particular importance to characterize the endogenous signaling profiles of that cell population. Cell seeding density, which can alter cell-cell distance, may be a critical parameter controlling subsequent cell proliferation and/or osteogenic signal expression due to changes in paracrine signaling distance among the cells. Furthermore, to determine the optimum seeding density for a specific type of scaffold (i.e., material substrate and surface geometry), it is imperative to stimulate sustained expression of some signals and not others. To this end, we aimed to investigate the effect of initial cell seeding density on the osteogenic gene expression of BMSCs on two dimensional crosslinked PPF disks. Two objectives were addressed in this study: (1) the effect of cell density on rat BMSC viability, proliferation, and osteogenic differentiation and (2) the effect of cell density on signalling profiles of osteogenic growth factors.

We first demonstrated the effect of cell seeding density on the attachment and viability of rat BMSCs (Figure 1). Although it is not possible to conclude there is a direct correlation between cell seeding density and the quality of attachment (or cell viability) from Figure 1, the extent of cellular attachment depends on surface properties of the substrate material. As cell attachment can be affected more by surface wettability and hydrophilicity rather than by surface topology [14], we observed that our PPF disk post-fabrication methods resulted in a suitable environment for the attachment of anchorage-dependent cells such as bone marrow stromal cells and osteoblasts.

Our next goal was to demonstrate the effect of cell seeding density on cell proliferation. As shown in recent literature, cell proliferation is strongly regulated by (1) surface area to allow attachment and (2) contact-inhibition between adjacent cells [22, 25, 32]. Although a highly interconnected porous scaffold is recommended to mimic the native bone, there remains a problem of achieving sufficient seeding efficiency. Alternatively, over-loaded cell numbers

may result in limiting nutrient transport, hypoxia of interior cells, and insufficient waste removal from the internal structures. Surface area dependence was also observed in our 2D study, as indicated by a proliferation rate that was lowest in the PPF Max groups (Figure 2). Distribution of rat BMSCs on PPF disks in Figure 1 indicates that lower cell seeding density resulted in a rapid proliferation rate over 8 days. Despite of the fact that high cellularity enhances cell-cell contact, contact-inhibition by gap junctional intercellular communication may suppress cell proliferation [33, 34]. As seen in a previously reported study [32], Figure 2 indicates that contact inhibition reduces cellular proliferation. As a result, we observed that 0.30 million cells per 18 mm diameter PPF disk was sufficient to induce contact inhibition and reduce rat BMSC proliferation rate.

Next, the effect of cell seeding density on the osteogenic differentiation of rat BMSCs was investigated. As a transient early osteogenic differentiation marker, ALP mRNA expression was measured (Figure 3). These data indicate that the PPF Med group exhibited statistically higher ALP expression on day 8 ($p = 1.75 \times 10^{-10}$) and that the PPF Max group showed the lowest expression level. It is known that ALP expression generally peaks prior to mineralization [35]. Since the ALP expression level in all groups peaked or started to plateau in the middle of the culture period, on day 4, it could be concluded that lower cell density induced early osteogenic differentiation of rat BMSCs after only 8 days. Therefore, it appears to be necessary to optimize rat BMSC cell density in order to stimulate the ALP expression on PPF disks.

Mineralization occurs late during the transition from cellular to osteoid tissue, following a sequential cascade of cell proliferation, ALP expression, and osteoblast phenotypic commitment (i.e., maturation) [36]. As a late marker of osteoid commitment, OC mRNA expression was assessed and calcium deposition was also measured (Figures 4 and 5). OC expression was seen to increase over 8 days and the PPF groups with higher seeding density (i.e., PPF Med and PPF Max) exhibited higher levels of OC expression; OC expression increased significantly in the TCPS Max also by day 8. OC expression, as seen in Figure 4, was consistent with the calcium deposition profile in Figure 5. Thus, the groups with higher cell seeding density presented higher levels of mineralization. Therefore, it would seem that late stage osteogenic differentiation was enhanced by higher cell seeding density, while cell proliferation and early osteogenic differentiation were stimulated by lower cell seeding density.

Our results indicate that three distinct periods in osteoblastic phenotype development may be sensitive to implant cell seeding density. According to the study by Lian and Stein [37], the first period of osteogenic progenitor cell growth exhibits strong proliferation with the formation of extracellular matrix. The second period shows matrix maturation with decreased cell proliferation, and upregulated ALP expression, a sequence of events also seen in our study. At these two stages, lower cell seeding density might enhance cellular proliferation and ALP expression due to reduced contact inhibition. In contrast, higher cell seeding density may stimulate mineralization, as is expected during the last period of osteoblast formation, along with downregulation of ALP activity and synthesis of osteopontin and bone proteoglycans such as decorin and biglycan. As described earlier, the rat BMSCs temporal growth pattern observed in this study agreed well with the expected cascade of bone formation events. Our observation also suggests that it may be possible to use cell seeding density to promote osteogenic differentiation in a 2D environment. However, optimization of cell seeding density needs to be tested in a 3D scaffold in order to confirm our hypothesis of the consistency between 2D and 3D microenvironments and the possibility of promoting the healing of bone wounds through the use of a tissue engineered implant.

Finally, qRT-PCR was performed to investigate the gene expression profile of endogenous growth factors relevant to bone formation, including BMP-2, FGF-2, TGF-β_1, and PDGF-A1. Natural bone matrix contains a number of growth factors and these growth factors play a critical role in proliferation, differentiation, and other cellular activities that are associated with these signaling molecules [38]. BMP-2 is one of the most investigated signaling molecules in the field of bone biology due to the following hypothesized roles: (1) regulation of cell growth, differentiation, apoptosis, and organ development, and (2) induction of osteoprogenitor cells found in bone fracture sites that are healing [39]. As shown in Figure 6A, the two lower density PPF groups had significantly higher BMP-2 expression than did the PPF Max group on day 1 ($p = 1.60 \times 10^{-7}$). The general trend of BMP-2 expression level over culture periods showed a decline on day 4 and then increased again by day 8. This expression pattern is the opposite of the ALP mRNA expression profile (i.e., peaked on day 4 and downregulated again by day 8), and this may be due to the opposing signal transduction for BMP-2 and ALP during early osteogenic differentiation. BMP-2 is thought to induce ALP production through Wnt expression and the Wnt/LRP5 signaling cascade [40]. Early expression of BMP-2 on day 1 might result in a BMP-2-rich extracellular environment. Subsequently, perhaps through the Wnt autocrine loop, ALP expression was observed to be downregulated by day 4 in our study. This expression profile can be found in other studies with 3D titanium scaffolds seeded with rat BMSCs [41] and 3D coralline hydroxyapatite scaffolds seeded with human mesenchymal stem cells (hMSC-TERT4) [35]. Interestingly, the PPF Med group showed higher expression of BMP-2 than the other two PPF groups on day 8, indicating that cell seeding density might be useful as a means to alter or optimize the BMP-2 expression of rat BMSCs.

It has been suggested that FGF-2 is associated with (1) regulation of skeletal growth and development including the balance between bone forming cells and bone resorbing cells, and (2) stimulation of osteoblasts by activating the Cbfa-1/Runx2 transcription factor [42, 43]. FGF-2 expression in Figure 6B was initially sustained on the PPF disks by day 4, but increased at day 8, showing significantly higher expression levels than in the TCPS groups. An increasing trend of FGF-2 expression at later time points may be due to Runx2-mediated signal transduction. FGF-2 expression is thought to activate Runx2 upregulation via the mitogen-activated protein kinase (MAPK) pathway, but Runx2 upregulation can also be induced by BMP-2 or TGF-β_1 stimulation via Smad and the MAPK intracellular signaling pathway [42, 44]. We also speculate that an early decline of BMP-2 expression may deactivate Runx2, and subsequently enhance FGF-2 expression in order to restore Runx2 activation via the MAPK pathway.

This hypothesis about the intracellular signaling pattern that is associated with growth factor signaling found during bone formation may also be applied to TGF-β_1 expression in Figure 6C. The decease in TGF-β_1 expression over time was similar to the BMP-2 expression profile, and it may also contribute to Runx2 deactivation and subsequent FGF-2 expression. This is consistent with the PPF Med groups on day 8 that presented statistically higher FGF-2 ($p = 3.35 \times 10^{-8}$) and TGF-β_1 ($p = 3.85 \times 10^{-9}$) expression levels. This result may suggest that over a period of 8 days rat BMSC cultures on PPF disks require an optimized cell density of approximately 75,000 cells per cm^2 (0.15 million cells/disk) to induce an optimal FGF-2 and TGF-β_1 expression profile that is compatible with bone formation. This may also suggest that there is an optimal cell seeding density for 3D scaffolds that is necessary to induce and/or promote the osteogenic differentiation and bone healing cascade.

Finally, it is also been observed that PDGF-A may stimulate DNA synthesis during in vitro bone formation [45]. In the present study, sustained PDGF-A mRNA expression was not correlated with DNA content (Figures 2 and 6D). However, the difference of PDGF-A

expression patterns over 8 days between the PPF and TCPS groups might indicate a substrate dependence in the expression of this growth factor.

Conclusions

The optimum level of bone progenitor cell seeding density for many different implant engraftment strategies is a critical issue for the clinical application of bone tissue engineering. The present study indicates that varying cell seeding density on PPF disks may be utilized to enhance the proliferation and differentiation of rat BMSCs. This study demonstrated (1) the effect of cell seeding density on viability, proliferation, and differentiation of rat BMSCs, and (2) the endogenous growth factor mRNA expression profiles of rat BMSCs on 2D PPF disks. The results of this study revealed that: (1) cell proliferation rate and early osteogenic differentiation were stimulated by a lower cell seeding density, (2) later differentiation, as indicated by mineralization, was enhanced by increasing cell seeding density, and (3) the temporal gene expression profiles of endogenous growth factors can be altered by initial cell seeding density.

Acknowledgments

This work was supported by the National Institutes of Health (R01-DE013740) and the National Science Foundation (CBET 0448684).

References

1. Baksh D, Song L, Tuan RS. J Cell Mol Med. 2004; 8(3):301–316. [PubMed: 15491506]
2. Jaiswal N, Haynesworth SE, Caplan AI, Bruder SP. J Cell Biochem. 1997; 64(2):295–312. [PubMed: 9027589]
3. Li WJ, Tuli R, Huang X, Laquerriere P, Tuan RS. Biomaterials. 2005; 26(25):5158–5166. [PubMed: 15792543]
4. Peter SJ, Liang CR, Kim DJ, Widmer MS, Mikos AG. J Cell Biochem. 1998; 71(1):55–62. [PubMed: 9736454]
5. Derubeis AR, Cancedda R. Ann Biomed Eng. 2004; 32(1):160–165. [PubMed: 14964731]
6. Salgado AJ, Coutinho OP, Reis RL. Macromol Biosci. 2004; 4(8):743–765. [PubMed: 15468269]
7. Shanti RM, Li WJ, Nesti LJ, Wang X, Tuan RS. J Oral Maxillofac Surg. 2007; 65(8):1640–1647. [PubMed: 17656295]
8. Shung AK, Timmer MD, Jo SB, Engel PS, Mikos AG. Journal of Biomaterials Science-Polymer Edition. 2002; 13(1):95–108. [PubMed: 12003078]
9. He S, Timmer MD, Yaszemski MJ, Yasko AW, Engel PS, Mikos AG. Polymer. 2001; 42(3):1251–1260.
10. Fisher JP, Timmer MD, Holland TA, Dean D, Engel PS, Mikos AG. Biomacromolecules. 2003; 4(5):1327–1334. [PubMed: 12959602]
11. Fisher JP, Holland TA, Dean D, Mikos AG. Biomacromolecules. 2003; 4(5):1335–1342. [PubMed: 12959603]
12. Fisher JP, Dean D, Mikos AG. Biomaterials. 2002; 23(22):4333–4343. [PubMed: 12219823]
13. Horch RA, Shahid N, Mistry AS, Timmer MD, Mikos AG, Barron AR. Biomacromolecules. 2004; 5(5):1990–1998. [PubMed: 15360315]
14. Lee KW, Wang S, Yaszemski MJ, Lu L. Biomaterials. 2008; 29(19):2839–2848. [PubMed: 18403013]
15. Peter SJ, Lu L, Kim DJ, Mikos AG. Biomaterials. 2000; 21(12):1207–1213. [PubMed: 10811302]
16. Shi XF, Hudson JL, Spicer PP, Tour JM, Krishnamoorti R, Mikos AG. Biomacromolecules. 2006; 7(7):2237–2242. [PubMed: 16827593]
17. Cooke MN, Fisher JP, Dean D, Rimnac C, Mikos AG. J Biomed Mater Res B Appl Biomater. 2003; 64(2):65–69. [PubMed: 12516080]

18. Lee JW, Lan PX, Kim B, Lim G, Cho DW. Microelectronic Engineering. 2007; 84(5–8):1702–1705.
19. Lee KW, Wang SF, Fox BC, Ritman EL, Yaszemski MJ, Lu LC. Biomacromolecules. 2007; 8(4): 1077–1084. [PubMed: 17326677]
20. Kempen DH, Lu L, Hefferan TE, Creemers LB, Maran A, Classic KL, Dhert WJ, Yaszemski MJ. Biomaterials. 2008; 29(22):3245–3252. [PubMed: 18472153]
21. Peter SJ, Lu L, Kim DJ, Stamatas GN, Miller MJ, Yaszemski MJ, Mikos AG. J Biomed Mater Res. 2000; 50(3):452–462. [PubMed: 10737888]
22. Ishaug SL, Crane GM, Miller MJ, Yasko AW, Yaszemski MJ, Mikos AG. J Biomed Mater Res. 1997; 36(1):17–28. [PubMed: 9212385]
23. Vehof JWM, de Ruijter AE, Spauwen PHM, Jansen JA. Tissue Eng. 2001; 7(4):373–383. [PubMed: 11506727]
24. Goldstein AS. Tissue Eng. 2001; 7(6):817–827. [PubMed: 11749737]
25. Bitar M, Brown RA, Salih V, Kidane AG, Knowles JC, Nazhat SN. Biomacromolecules. 2008; 9(1):129–135. [PubMed: 18095652]
26. Kruyt M, de Bruijn J, Rouwkema J, Clemens VB, Oner F, Verbout A, Dhert W. Tissue Eng Part A. 2008
27. Zhou YF, Sae-Lim V, Chou AM, Hutmacher DW, Lim TM. J Biomed Mater Res A. 2006; 78(1): 183–193. [PubMed: 16628549]
28. Lieb E, Vogel T, Milz S, Dauner M, Schulz MB. Tissue Eng. 2004; 10(9–10):1414–1425. [PubMed: 15588401]
29. Maegawa N, Kawamura K, Hirose M, Yajima H, Takakura Y, Ohgushi H. J Tissue Eng Regen Med. 2007; 1(4):306–313. [PubMed: 18038421]
30. van den Dolder J, de Ruijter AJ, Spauwen PH, Jansen JA. Biomaterials. 2003; 24(11):1853–1860. [PubMed: 12615475]
31. van der Zande M, Walboomers XF, Briest A, Springer M, Alava JI, Jansen JA. J Biomed Mater Res A. 2008; 86(3):788–795. [PubMed: 18041723]
32. Toh YC, Ho ST, Zhou Y, Hutmacher DW, Yu H. Biomaterials. 2005; 26(19):4149–4160. [PubMed: 15664642]
33. Banoub RW, Fernstrom M, Ruch RJ. Cancer Lett. 1996; 108(1):35–40. [PubMed: 8950206]
34. van den Dolder J, Spauwen PH, Jansen JA. Tissue Eng. 2003; 9(2):315–325. [PubMed: 12740094]
35. Mygind T, Stiehler M, Baatrup A, Li H, Zou X, Flyvbjerg A, Kassem M, Bunger C. Biomaterials. 2007; 28(6):1036–1047. [PubMed: 17081601]
36. Owen TA, Aronow M, Shalhoub V, Barone LM, Wilming L, Tassinari MS, Kennedy MB, Pockwinse S, Lian JB, Stein GS. J Cell Physiol. 1990; 143(3):420–430. [PubMed: 1694181]
37. Lian JB, Stein GS. Crit Rev Oral Biol Med. 1992; 3(3):269–305. [PubMed: 1571474]
38. Li RH, Wozney JM. Trends Biotechnol. 2001; 19(7):255–265. [PubMed: 11412949]
39. Kirker-Head CA. Adv Drug Deliv Rev. 2000; 43(1):65–92. [PubMed: 10967222]
40. Rawadi G, Vayssiere B, Dunn F, Baron R, Roman-Roman S. J Bone Miner Res. 2003; 18(10): 1842–1853. [PubMed: 14584895]
41. Pham QP, Kurtis Kasper F, Scott Baggett L, Raphael RM, Jansen JA, Mikos AG. Biomaterials. 2008; 29(18):2729–2739. [PubMed: 18367245]
42. Franceschi RT, Xiao G. J Cell Biochem. 2003; 88(3):446–454. [PubMed: 12532321]
43. Mackay AM, Beck SC, Murphy JM, Barry FP, Chichester CO, Pittenger MF. Tissue Eng. 1998; 4(4):415–428. [PubMed: 9916173]
44. Lee KS, Hong SH, Bae SC. Oncogene. 2002; 21(47):7156–7163. [PubMed: 12370805]
45. Canalis E, McCarthy TL, Centrella M. J Cell Physiol. 1989; 140(3):530–537. [PubMed: 2777891]

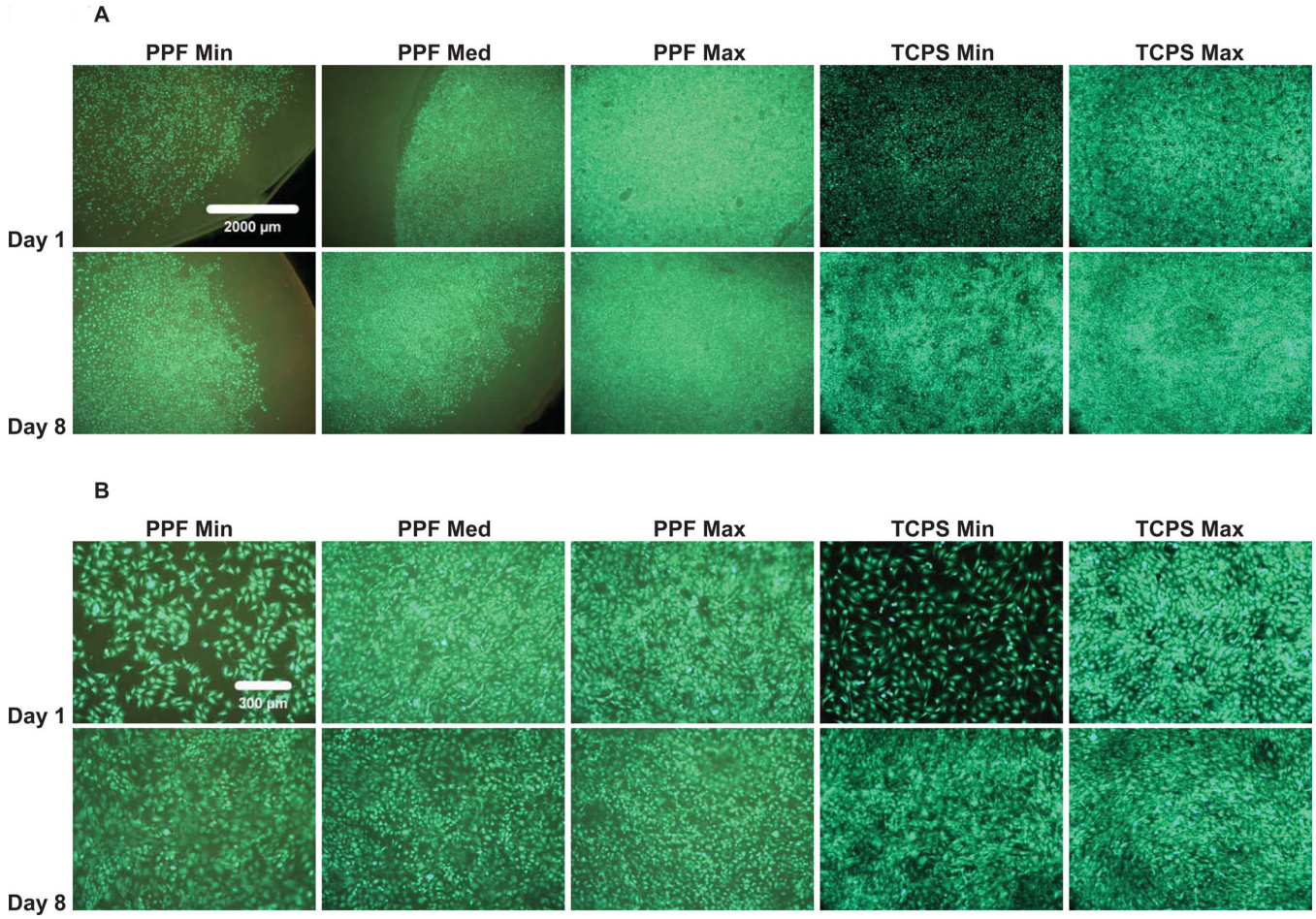

Figure 1.

Qualitative Live/Dead fluorescent staining images with a 2.5x magnification in (A) and 10x magnification in (B) of PPF disks and TCPS well plates (positive control). The result demonstrated that rat BMSCs are viable over an 8 day culture period in all experimental groups. The fluorescent images also qualitatively demonstrated a similar attachment pattern and viability of rat BMSCs on PPF disks compared with the control groups. The scale bar shown in 1A represents 2000 μm and applies to all images. The scale bar in 1B represents 300 μm and applies to all images.

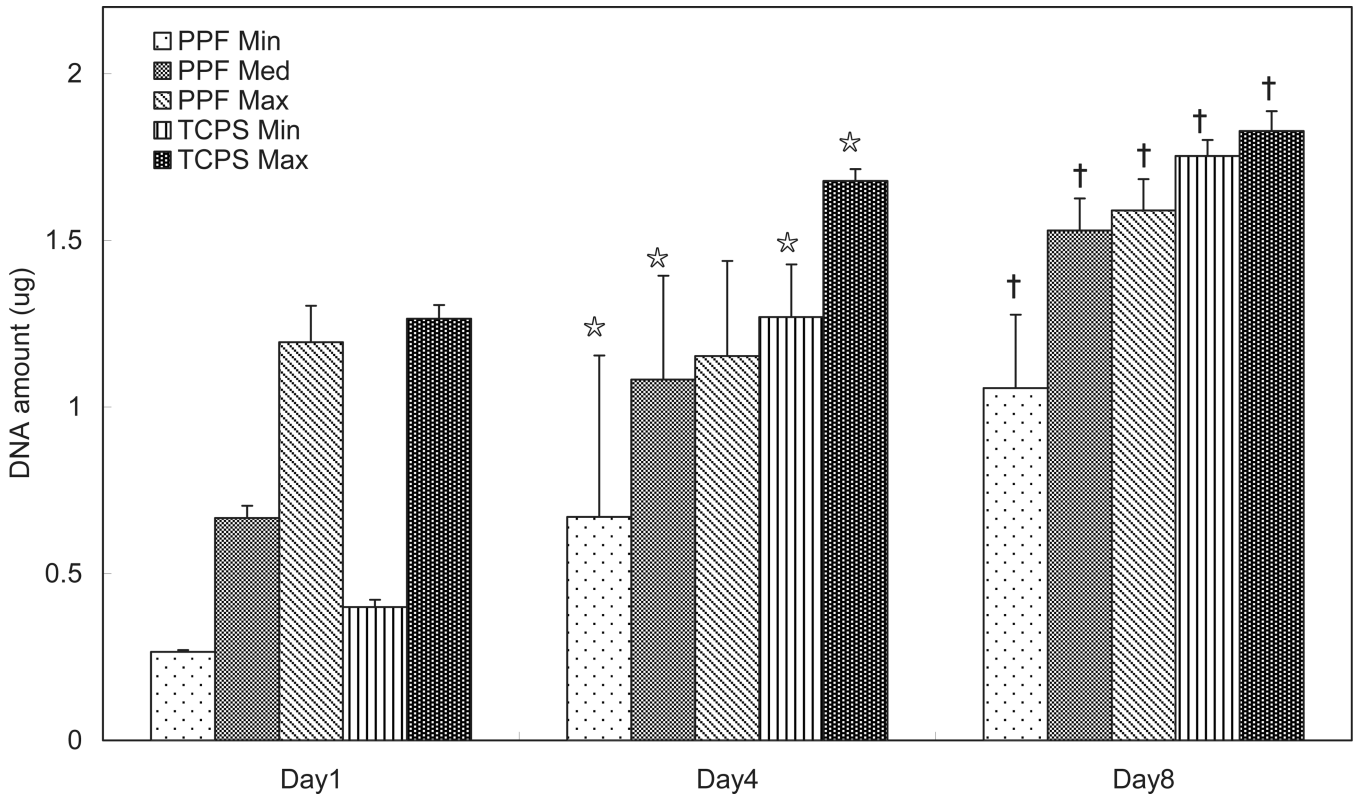

Figure 2.

The quantitative DNA amount represents levels of cellular proliferation on the 2D PPF disks and TCPS groups over the course of 8 days (n=3 per group). The DNA amount per experimental group is shown in μg per disk and as average ± standard deviation. ☆ indicates a statistical difference compared to data on day 1 while † indicates a statistical difference compared to data on day 4 in each experimental group ($p<0.05$).

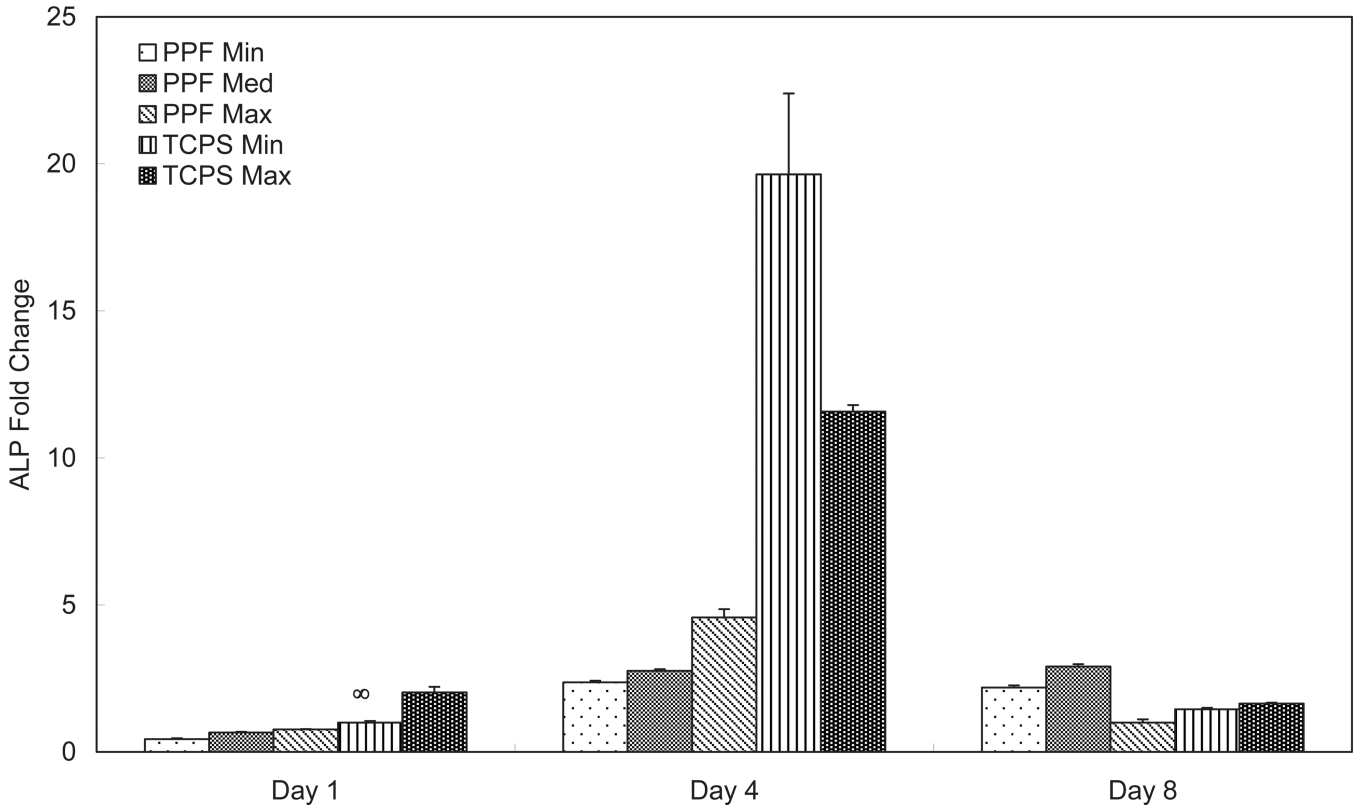

Figure 3.
Quantitative RT-PCR analysis of gene expression profiles of ALP osteogenic differentiation markers for 1, 4, and 8 days. The fold changes in gene expression level are reported as average ± standard deviation (n=3) and the calibrator for all experimental groups is indicated by a ∞ marker.

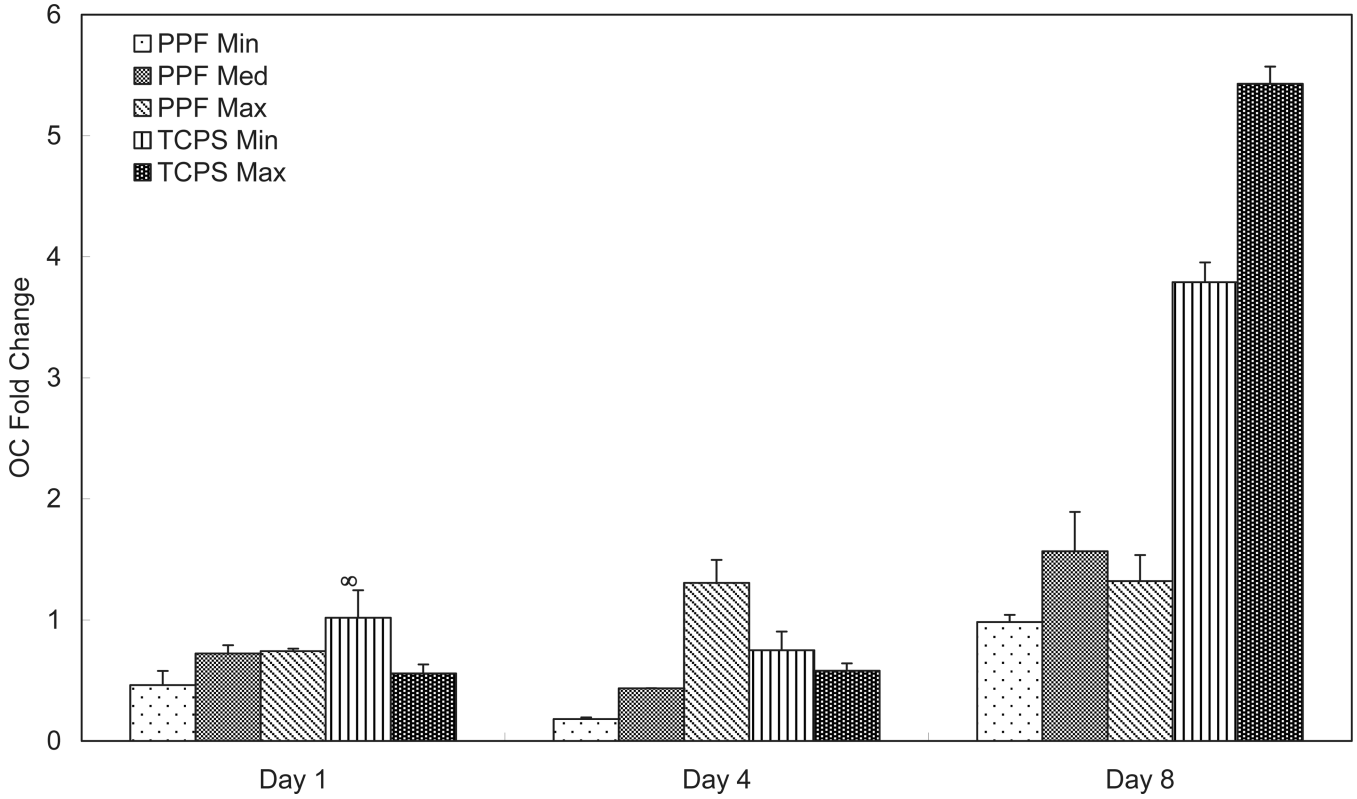

Figure 4.
Quantitative RT-PCR analysis of gene expression profiles of OC osteogenic differentiation markers for 1, 4, and 8 days. The fold changes in gene expression level are reported as average ± standard deviation (n=3) and the calibrator for all experimental groups is indicated by a ∞ marker.

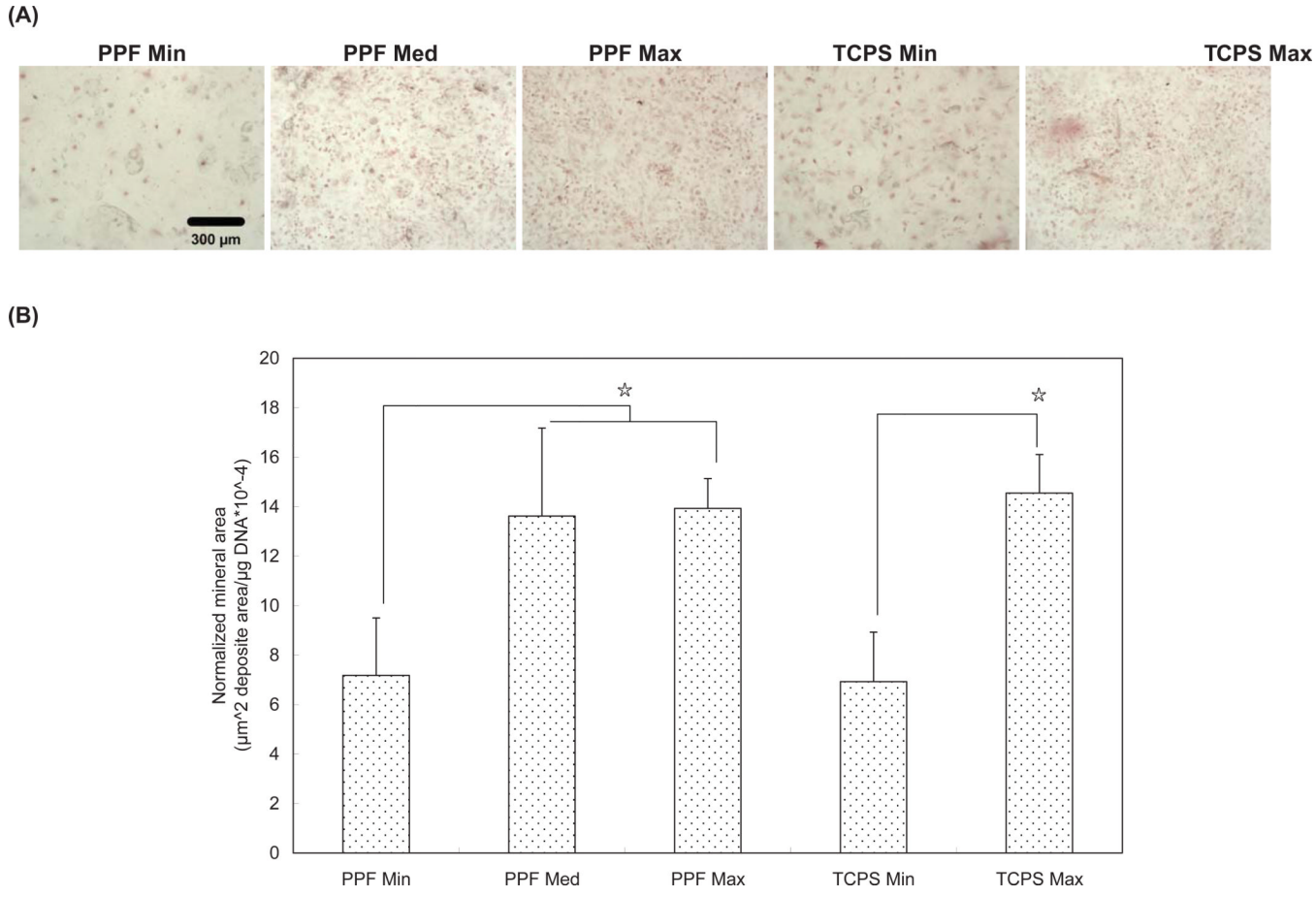

Figure 5.

Mineralization assay by Alizarin Red S staining at Day 8. (A) Qualitative light microscopy images of calcium deposits in rat BMSCs. The scale bar represents 300 μm and applies to all images. (B) Normalized calcium deposition. ☆ indicates a statistical difference between groups ($p<0.05$).

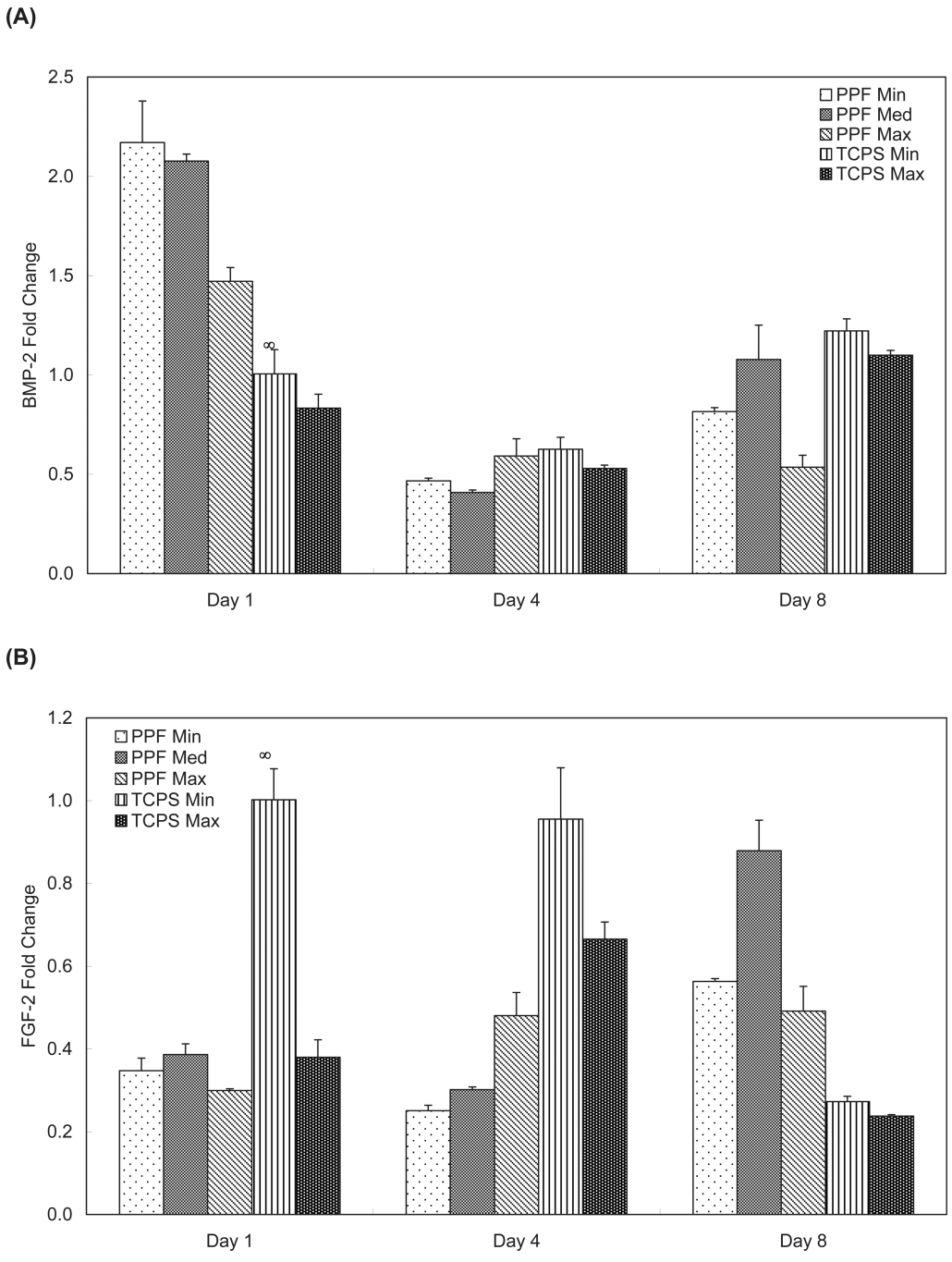

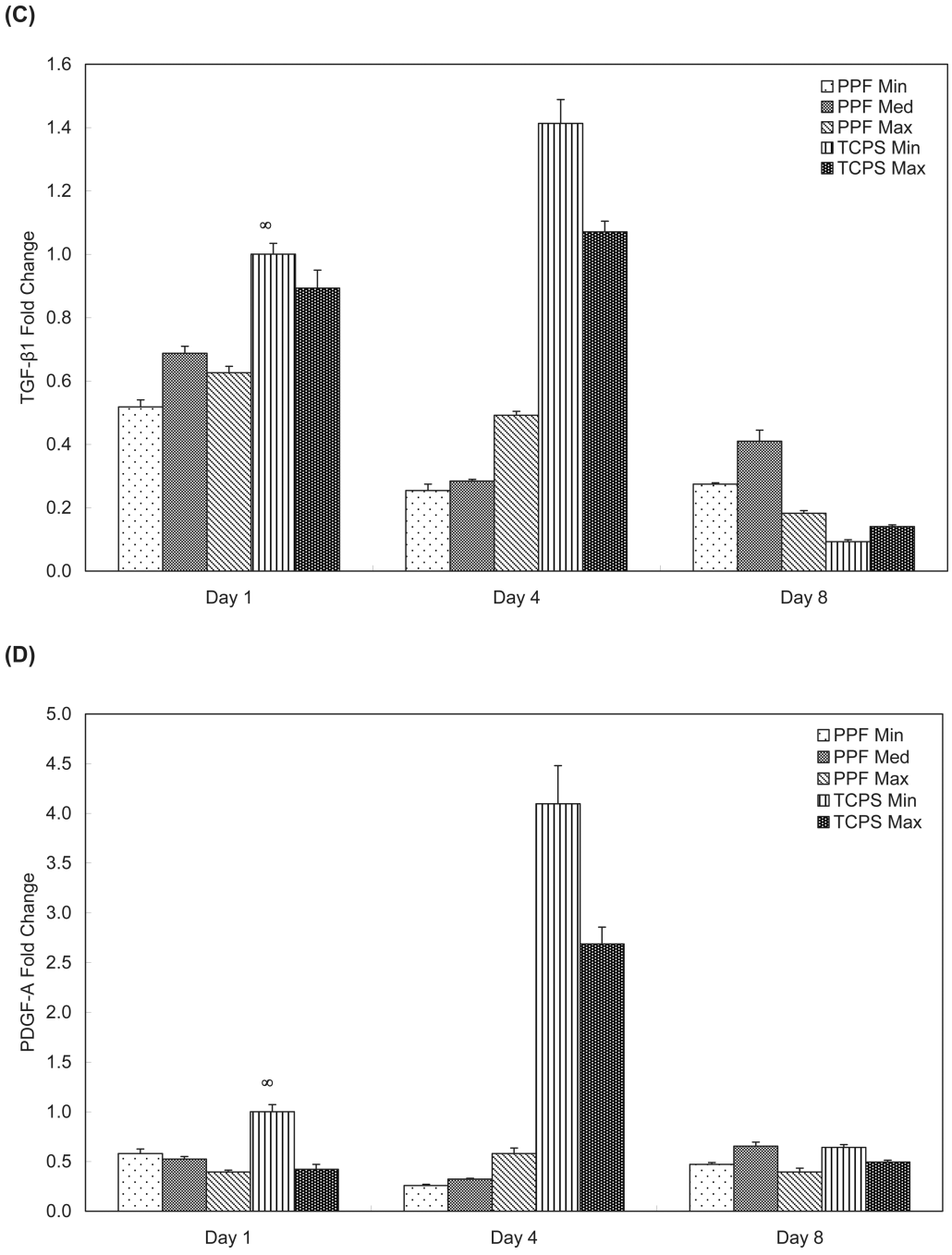

Figure 6.

Quantitative RT-PCR analysis of gene expression profiles of growth factors (A: BMP-2, B: FGF-2, C: TFG-β_1, and D: PDGF-A) for 1, 4, and 8 days. The fold changes in gene expression level are reported as average ± standard deviation (n=3) and the calibrator for all experimental groups is indicated by a ∞ marker.

Table 1

Experimental and Control Groups

Groups	Description	Cell Density (cells/cm^2)
PPF Min	60,000 cells on PPF disk	30,000
PPF Med	150,000 cells on PPF disk	75,000
PPF Max	300,000 cells on PPF disk	149,000
TCPS Min	60,000 cells per well of tissue culture polystyrene 12 well plate	30,000
TCPS Max	300,000 cells per well of tissue culture polystyrene 12 well plate	149,000